Rockslope stability analysis – an overview

Authors: Prof. Dr. habil. Heinz Konietzky (TU Bergakademie Freiberg, Geotechnical Institute)

Editor: Prof. Dr.-Ing. habil. Heinz Konietzky Layout: Angela Griebsch
TU Bergakademie Freiberg, Institut für Geotechnik, Gustav-Zeuner-Straße 1, 09599 Freiberg • sekr_fm@ifgt.tu-freiberg.de

1 Introduction

Instability (failure) of rock slopes is mainly governed by one of the foland owing mechanisms:

- Wedge failure by two discontinuities in which intersection lines dip towards the slope
- Toppling of rock columns or slabs created by vertical discontinuities close to the slope
- Circular slip surfaces in heavily jointed / fractured rocks masses
- Rockfall of loose blocks due to slipping, rolling or toppling
- Planar failure along discontinuities dipping in the direction of the slope

Key factors affecting the slope stability are:

- Geometry of slope
- Geometry and orientation of planes of weakness (joints, faults, cracks etc.)
- Properties of planes of weakness (cohesion, friction, fillings, roughness etc.)
- Water pressure (joint and pore water pressure)
- Additional loads (static or dynamic)

In terms of the geometry we can distinguish between planar, circular, piece-wise planar, non-circular and composite failure surfaces (see Fig. 1.1).

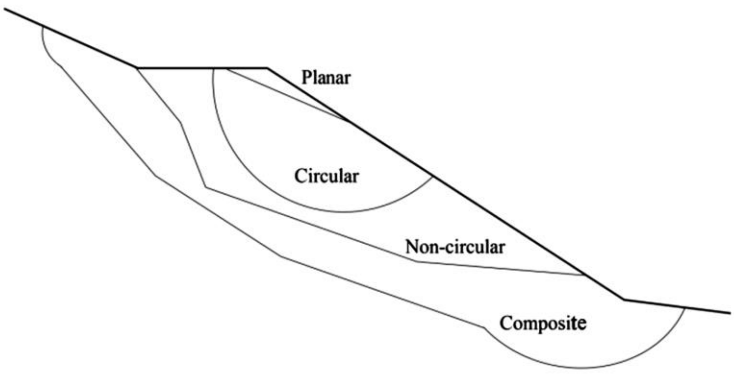

Fig. 1.1: Different types of slip surfaces

2 Analysis methods

In principle the following methods / tools are available to determine or estimate the slope stability:

- Analytical solutions for simple constellations considering mechanical equilibrium
- Kinematic assessment of potential failure along discontinuities (wedge analysis)
- Empirical approaches based on rock mass classification schemes
- Limit equilibrium methods
- Numerical methods

2.1 Analytical Solutions

Simple analytical solutions can be obtained by considering force and/or moment equilibrium. The following three pictures give examples.

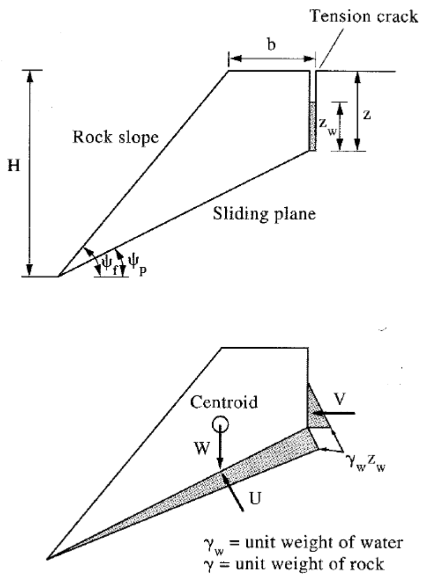

$$SF = \frac{c'(H-z)\csc\psi_p + (W\cos\psi_p - U - V\sin\psi_p)\tan\phi'}{V\cos\psi_p + W\sin\psi_p}$$

Where:

SF = safety factor
c' = effective cohesion
ϕ' = effective friction angle
ψ_p = dip of slide plane
W = weight of block
U = uplift force due to water pressure along slide plane
V = force due to water pressure in tension crack
H = slope height
z = tension crack depth

Fig. 2.1.1: Analytical planar failure analysis (Eberhardt, 2003)

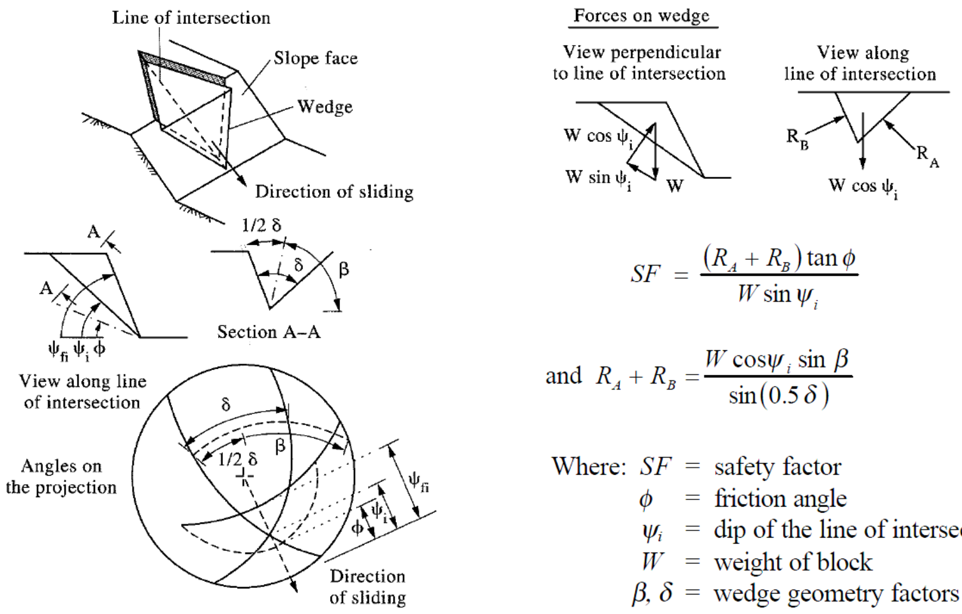

$$SF = \frac{(R_A + R_B)\tan\phi}{W\sin\psi_i}$$

$$\text{and } R_A + R_B = \frac{W\cos\psi_i \sin\beta}{\sin(0.5\,\delta)}$$

Where: SF = safety factor
ϕ = friction angle
ψ_i = dip of the line of intersection
W = weight of block
β, δ = wedge geometry factors

Fig. 2.1.2: Analytical wedge failure analysis (Eberhardt, 2003)

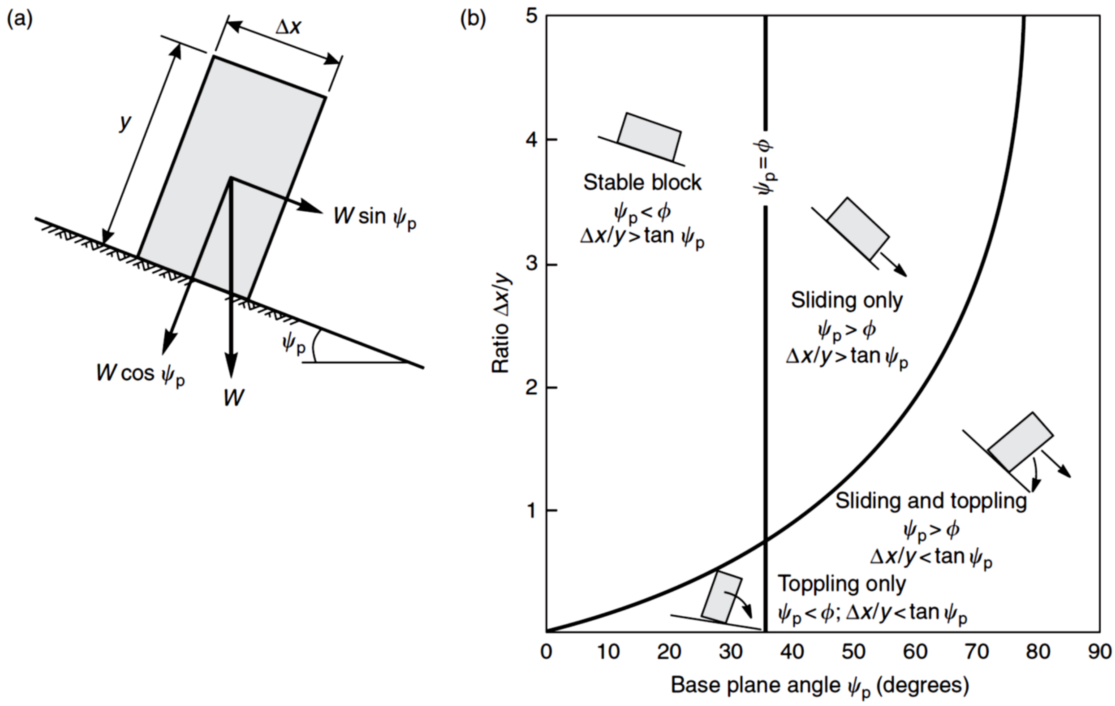

Fig. 2.1.3: Analytical solution for identification of sliding vs. toppling (Wyllie & Mah, 2005)

2.2 Kinematic analysis

Kinematic analysis proofs if slope failure is kinematic possible as planar or wedge type failure. Classical analysis considers weight of the potential failed rock block, friction as well as cohesion, some tools consider also additional tensile cracks. The analysis can be performed deterministic (consideration only of individual detected joints, faults etc.) or in a stochastic manner considering joint sets with certain span in orientation (Monte-Carlo type of simulation).
The kinematic analysis allows to determine potential failures for single blocks (Fig. 2.2.1). However, this method has certain restrictions: it does not consider the complex 3D stress field in a slope and it does not consider complex failure types. Fig. 2.2.2 shows the result of a wedge failure analysis for a rock slope with three joint sets. The potential failed rock blocks created by crossing joints assuming a friction angle of 27° (zero cohesion) for a slope dip of 74° are shown in red using a stereographic projection.

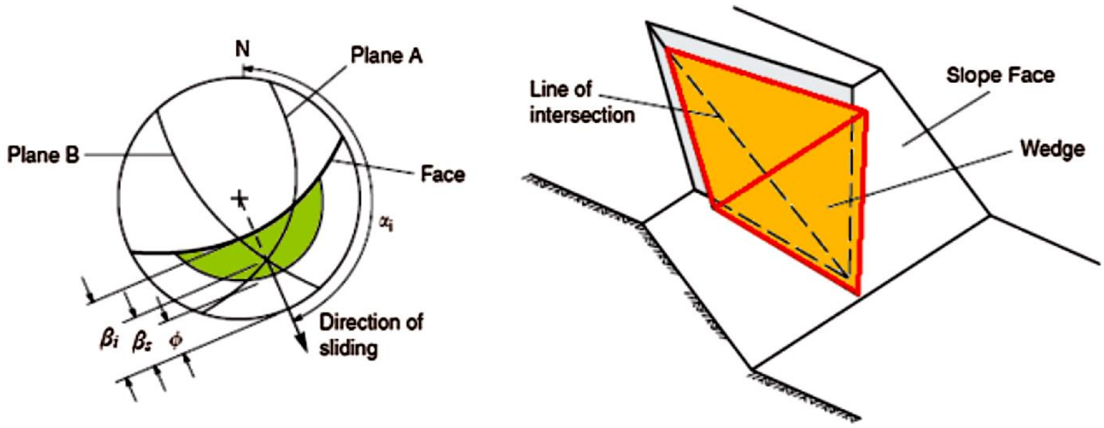

Fig. 2.2.1: Principle of kinematic wedge analysis for slopes (Rusydy et al., 2019)

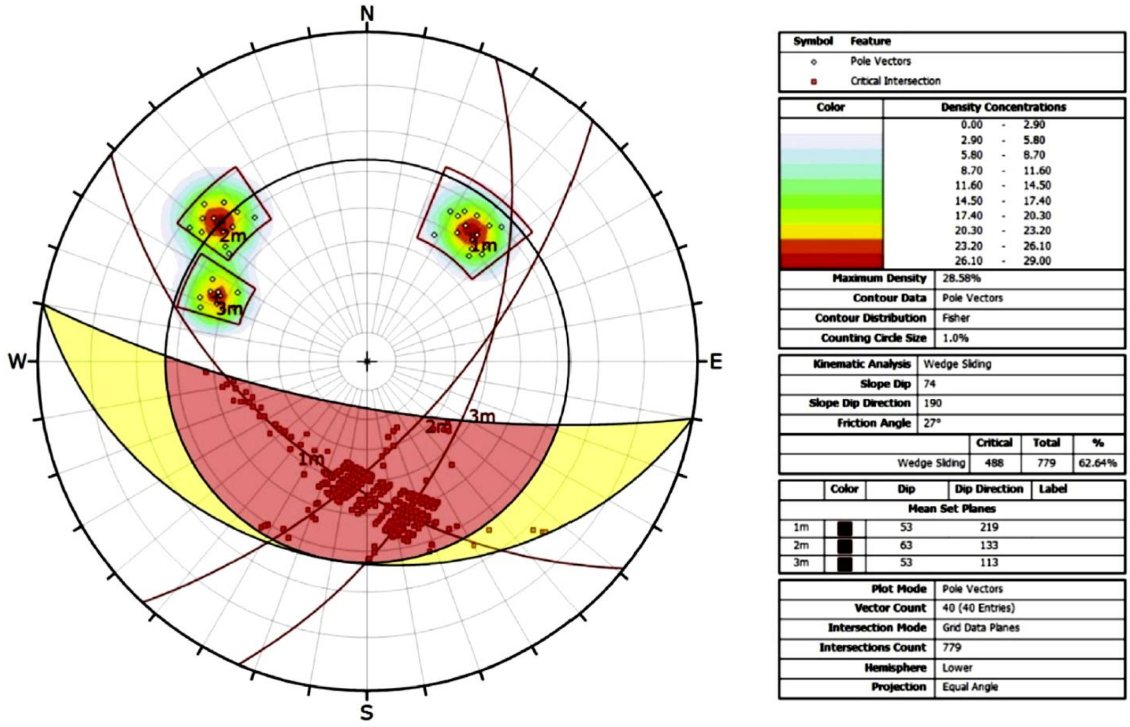

Fig. 2.2.2: Example of wedge failure analysis with 3 joint sets (Basahel & Mitri, 2017)

2.3 Empirical approaches based on rock mass classification

Based on field observations (case histories) several authors have developed design charts for slopes on the basis of rock mass classifications. Fig. 2.3.1 shows an example using the GSI classification system. Based on a modified GSI classification scheme according to Fig. 2.3.2, Taheri & Tani (2007) propose a slope stability design chart (Fig. 2.3.4) based on a rating according to Fig. 2.3.3 (SSR = Slope Stability Rating). Bar & Barton (2017) have analyzed more than 400 case histories using the Q-slope system (see Fig. 2.3.5) and deduced a design chart like shown in Fig. 4.3.3. Sonmez & Ulusay (1999) proposed a modified GSI classification scheme for slopes (see Fig. 2.3.2). The most popular rock mass classification for slopes is the so-called ‘Slope Mass Rating – SMR’ based on the RMR system:

$$SMR = RMR + (F_1 \cdot F_2 \cdot F_3) + F_4 \qquad (2.3.1)$$

where F_1 to F_4 are specific values characterizing the discontinuities as well as the excavation method (Romana et al., 2015).

The Q-slope value is determined using the following modification of the Q-System:

$$Q_{slope} = \frac{RQD}{J_n} \cdot \frac{J_r}{J_a} \cdot \frac{J_{w,ice}}{SRF_{slope}} \qquad (2.3.2)$$

where $J_{w,ice}$ and SRF_{slope} are modified Q-system parameters (see Bar & Barton, 2017).

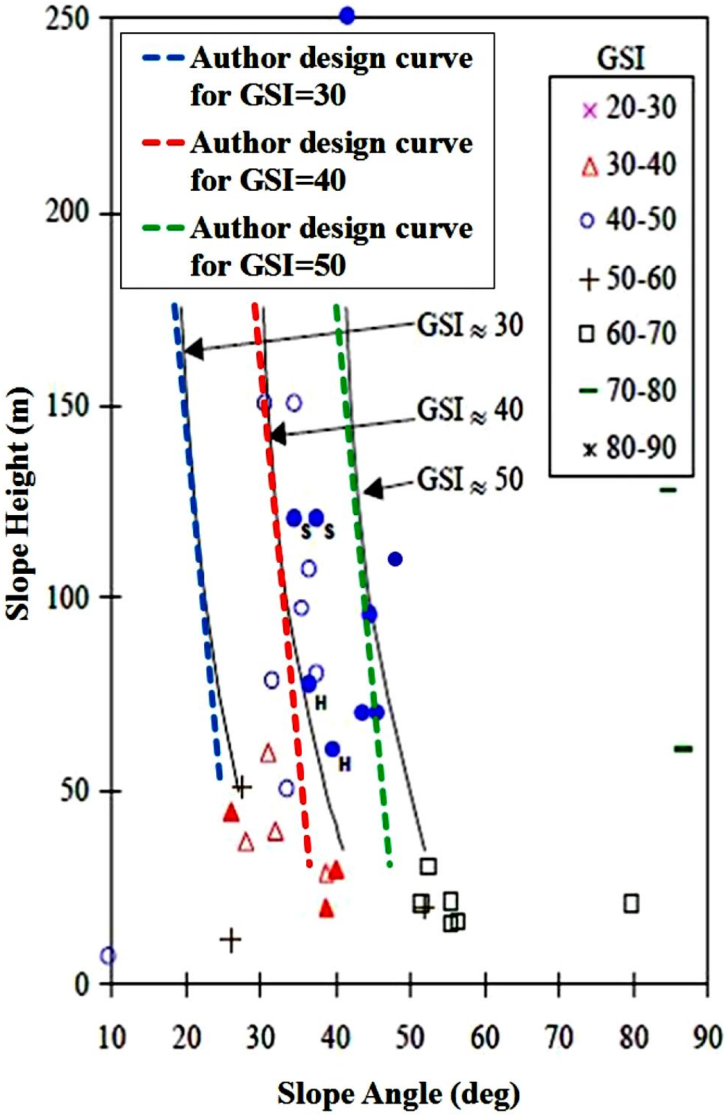

Fig. 2.3.1: Wet slope stability design chart; solid symbols indicate unstable slopes (Wattimena, 2013)

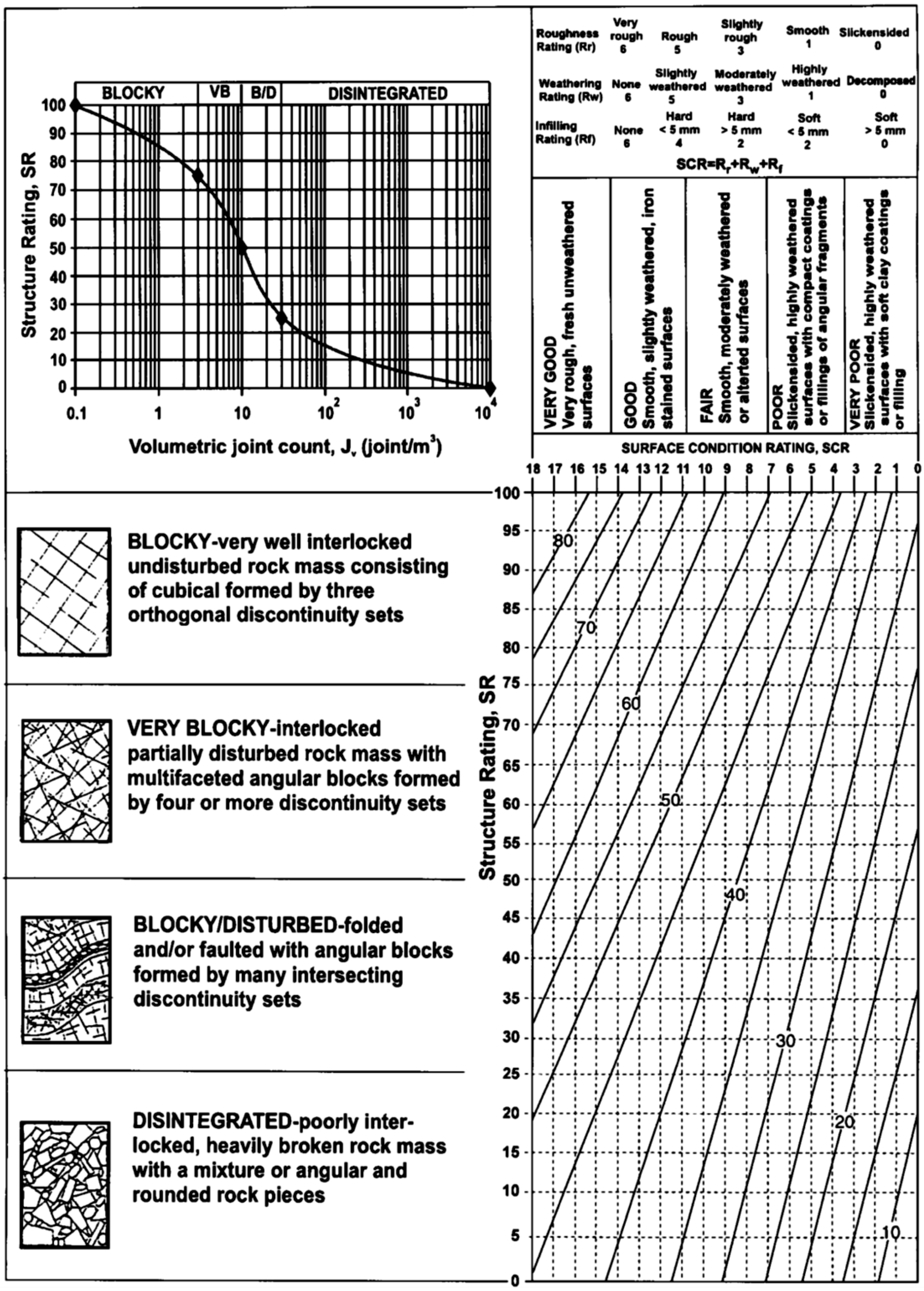

Fig. 2.3.2: Modified GSI classification for rock slope analysis (Sonmez & Ulusay, 1999)

Parameter		Range of values					
1	Modified GSI	(Refer to Fig. 1)					
	Rating	0 - 100					
2	Uniaxial compressive strength (MPa)	0 -10	10 -25	25 - 50	50 - 100	100 - 150	150 - 200
	Rating	0	7	18	28	37	43
3	Rock type (Refer to Table 2)	Group 1	Group 2	Group 3	Group 4	Group 5	Group 6
	Rating	0	4	9	17	20	25
4	Slope excavation method	Waste damp	Poor blasting	Normal blasting	Smooth blasting	Pre-splitting	Natural slope
	Rating	-11	-4	0	6	10	24
5	Ground-water: Groundwater level from slope toe / Slope height *100	Dry	0 – 20%	20 – 40%	40 – 60%	60 - 80%	80 – 100%
	Rating	0	-1	-3	-6	-14	-18
6	Earthquake force: Horizontal acceleration	0	0.15 g	0.20 g	0.25 g	0.30 g	0.35 g
	Rating	0	-11	-15	-19	-22	-26

Group	Rock type	Name of rocks
1	Sedimentary	Clay Shale, Mudstone, Claystone & Marl
	Igneous	Highly weathered, sheared, or altered rocks
2	Metamorphic	Schists & Mylonites
3	Sedimentary	Limestone Shale, Dolomite, Limestone, Chalk & Siltstone
	Metamorphic	Slate, Phyllites & Marble
4	Sedimentary	Anhydrite & Gypsum
	Igneous	Tuff, Basalt, Breccia, Dacite & Rhyolite
5	Sedimentary	Breccia, Greywacke, Sandstone & Conglomarate
	Metamorphic	Hornfels
	Igneous	Dolerite, Obsidian, Andesite, Norite & Agglomerate
6	Igneous	Granite, Granodiorite, Diorite & Gabbro

Fig. 2.3.3: Rating scheme for modified GSI classification scheme (Taheri & Tani, 2007)

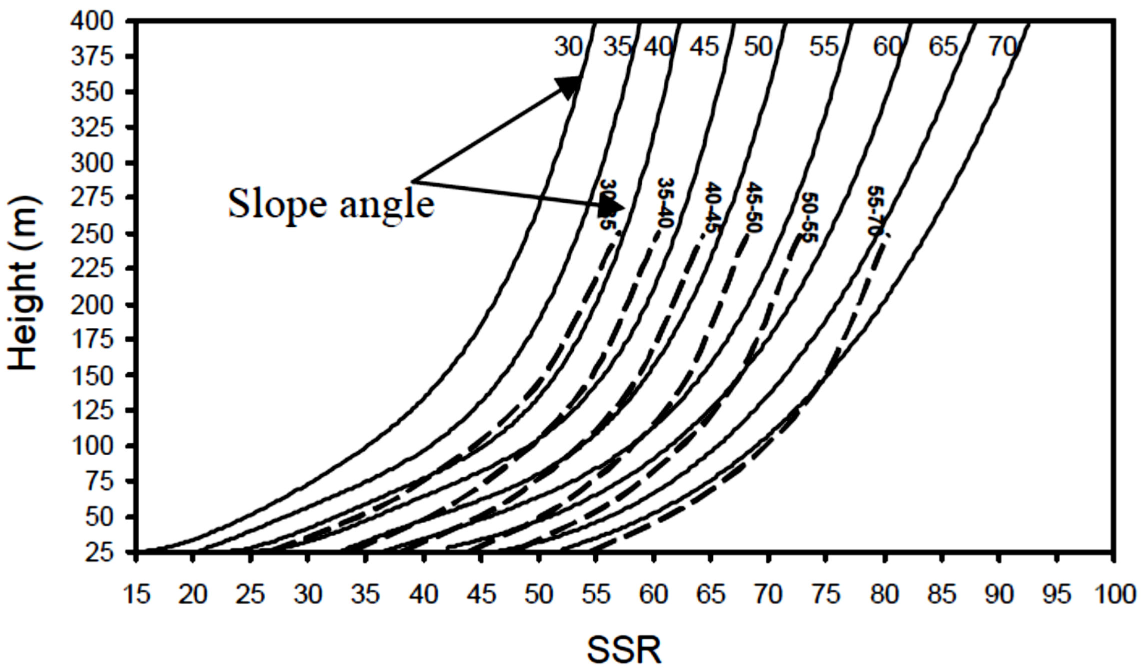

Fig. 2.3.4: Comparison between original and modified slope design charts (Taheri & Tani, 2007)

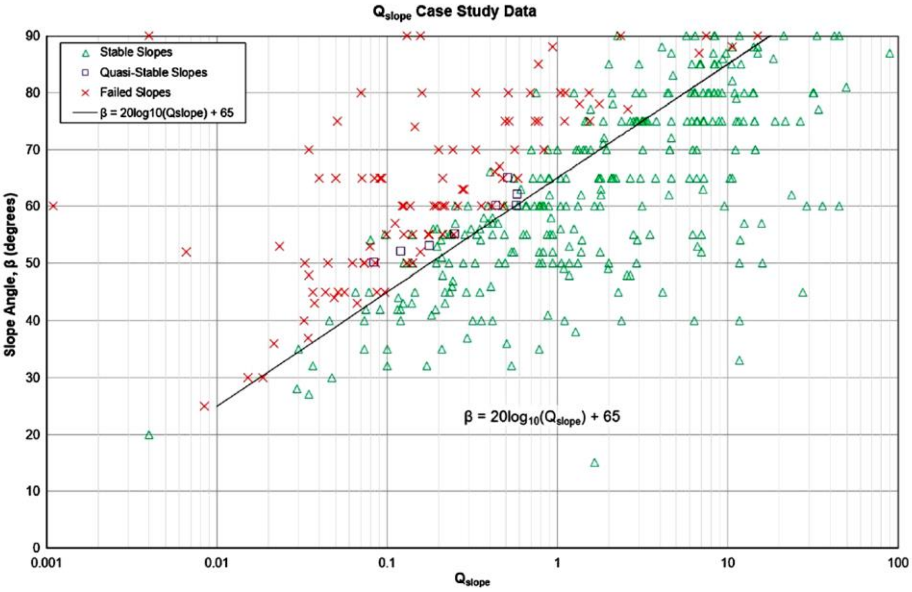

Fig. 2.3.5: Q-slope data for 412 case histories: stable vs. unstable slopes (Bar & Barton, 2017)

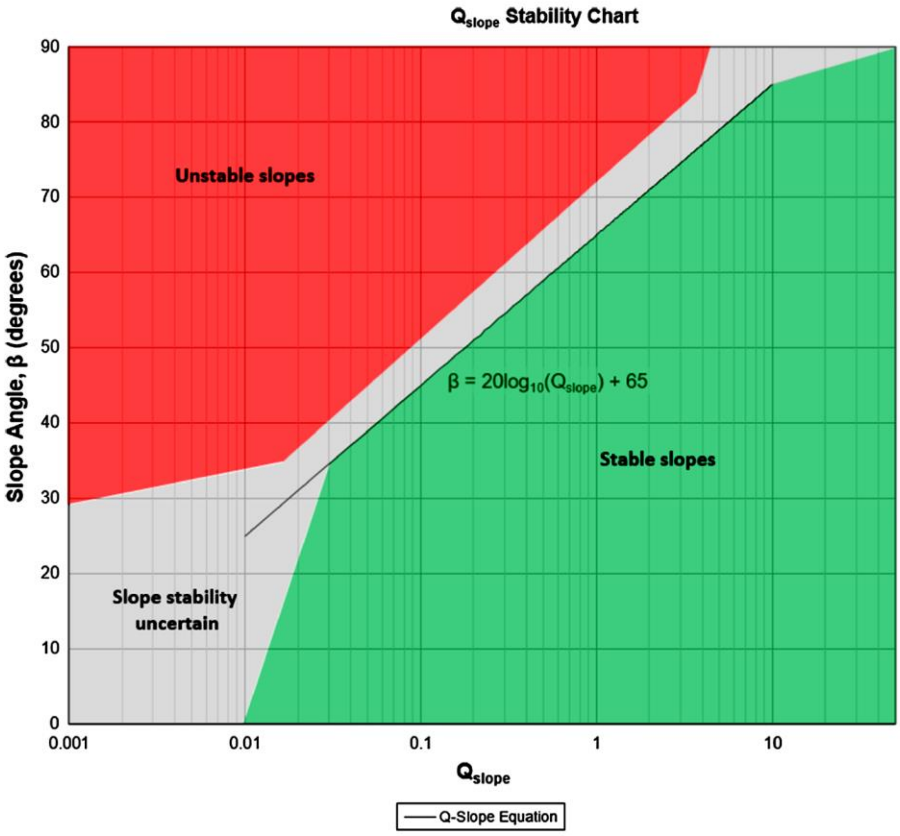

Fig. 2.3.6: Q-slope stability chart (Bar & Barton, 2017)

Li et al. (2008) have performed systematic numerical slope stability analysis using the Hoek-Brown failure criterion (see Fig. 2.3.7). Depending on rock type m_i, UCS of intact rock, slope height and angle as well as specific weight and safety factor F the stability of a rock slope for different GSI-values can be obtained.

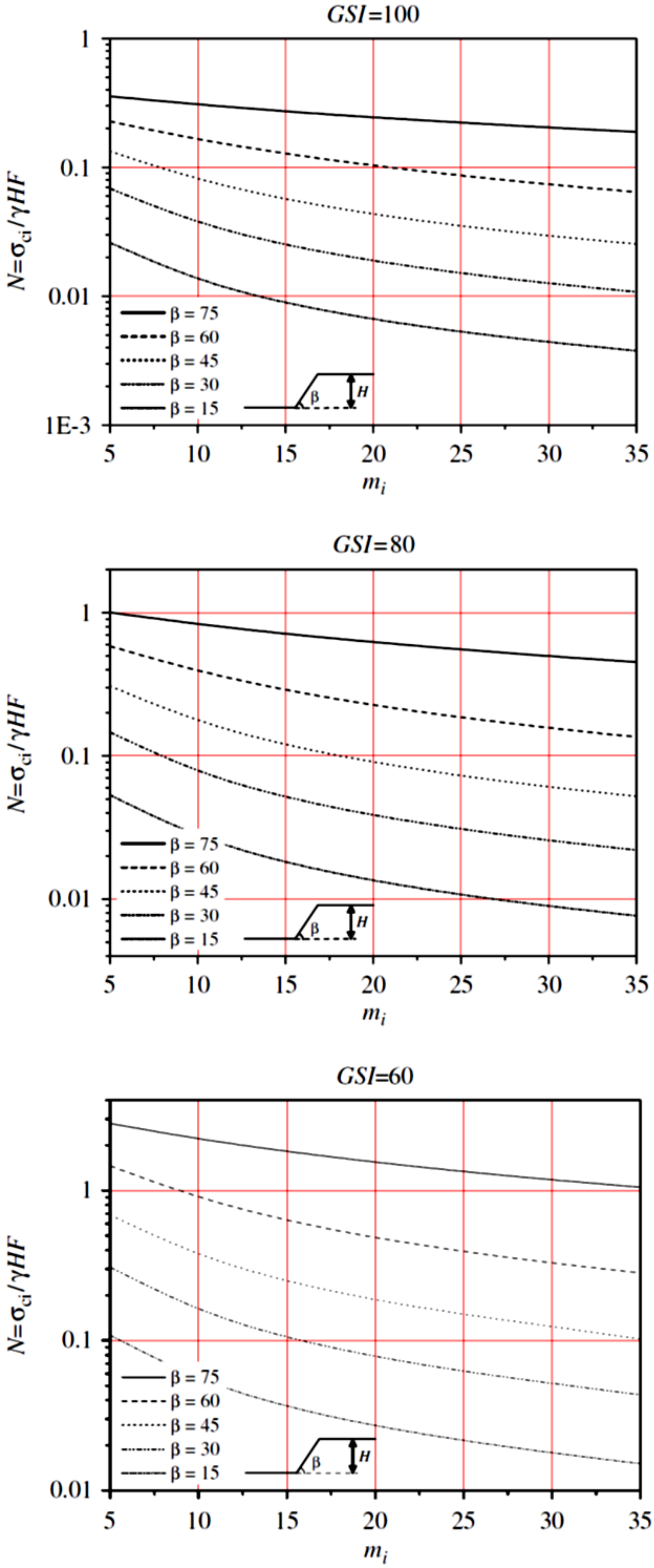

Fig. 2.3.7: Stability chart for slopes using Hoek-Brown failure criterion (Li et al., 2008)

Haines & Terbrugge (1991) have set-up an empirical slope design chart which indicates areas where design based on rock mass classification may be sufficient or not (see Fig. 2.3.8).

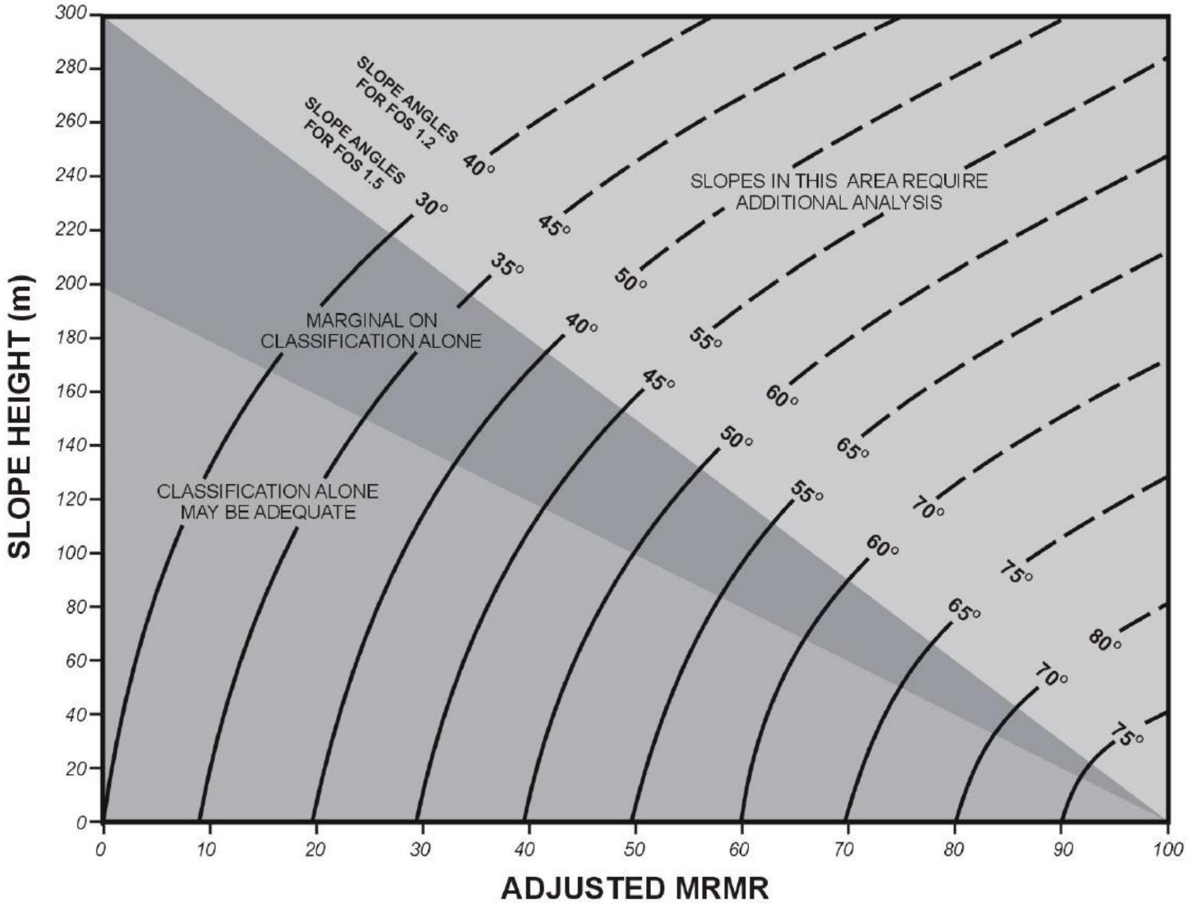

Fig. 2.3.8: Empirical slope design chart (Haines & Terbrugge, 1991)

2.4 Limit equilibrium methods

Limit equilibrium methods consider force and/or moment equilibrium for a slope. For the calculation the slope is split into slices or blocks. Considered failure mechanisms and slip surfaces can be quite different as documented by Tab. 2.4.1.

LEMs	Equilibrium conditions satisfied	Slip surface	Failure mechanism	Application	References
OMS/Fellenius method	Moment equilibrium about the circle center	Circular	Rotational	Mass/Slice approach	Fellenius (1936)
Simplified Bishop method	Vertical force equilibrium and moment equilibrium about the center	Circular	Rotational	Mass/Slice approach	Bishop (1955)
Extended Bishop method	Moment equilibrium about the center	Circular	All	Mass/Slice approach	Nonveiller (1965)
Lorimer method	Vertical force equilibrium and moment equilibrium about the center	Circular	All	Slice approach	Fredlund, Krahn, and Pufahl (1981)
Simplified Janbu method	Vertical and horizontal force equilibrium and shear interslice force is assumed ZERO	General shape	All	Mass/Slice approach	Janbu (1954)
Modified Swedish method	Vertical and horizontal force equilibrium	General shape	All	Slice approach	USACE (2003)
USACE's 1970 procedure	Vertical and horizontal force equilibrium and interslice force inclination is parallel with ground	General shape	All	Slice approach	USACE (2003)
Lowe–Karafiath method	Horizontal and vertical force equilibrium and interslice force inclination is equal with slip and ground surfaces	General shape	All	Slice approach	Lowe and Karafiath (1960)
Sarma method I	Vertical and horizontal force equilibrium and shear strength on the interface between adjacent slices and	General shape	All	Slice approach	Sarma (1979)
Spencer method	Rigorous limiting equilibrium and interslice force inclination is constant	General shape	All	Slice approach	Spencer (1967)
Morgenstern – Price method	Rigorous equilibrium by interslice force function	General shape	All	Slice approach	Morgenstern and Price (1965)
Sarma method II and III	Rigorous equilibrium of extended Sarma method I	General shape	All	Slice approach	Sarma (1973)
Correia method	Rigorous equilibrium and shear interslice force described by shapes function and force dimension	General shape	All	Slice approach	Correia (1988)
Rigorous Janbu method	All the force and moment conditions are equilibrium	General shape	All	Slice approach	Janbu (1954); Janbu, Bjerrum, and Kjaernsli (1956)
USACE's 2003 procedure	Improvement of USACE's 1970 procedure	General shape	All	Slice approach	USACE (2003)
Wedge method	Fully satisfies the vertical and horizontal force equilibrium	General shape	Wedge	Zone approach	Abramson et al. (2001)
Infinite slope method	Horizontal and vertical force equilibrium	Planar	Plane	Critical circle	USACE (2003)
Planar failure analysis	Horizontal and vertical force equilibrium	Planar	Plane	Geometry controlled	Hoek and Bray (1981)
Wedge failure analysis	Horizontal and vertical force equilibrium	Wedge	Wedge	Geometry controlled	Brady and Brown (2005)
Circular failure analysis	Horizontal and vertical force equilibrium	Circular	Rotational	Mass/Slice approach	Wyllie and Mah (2004)
Toppling failure analysis	Vertical and horizontal force equilibrium and moment equilibrium	Rotation	Toppling	Geometry controlled	Freitas and Watters (1973)
Block theory	Geometrical equilibrium and force/ moment vectors equilibrium	General shape	All	Geometry controlled	Goodman and Shi (1985)

Fig. 2.4.1: Overview about limit equilibrium methods for slope stability analysis (Azarafza et al., 2021)

2.5 Numerical simulations

Numerical stability calculations for slopes can be performed in three different ways:

- via classical continuum based approaches (mainly FEM or FDM) using rock mass parameters, which may include the consideration of smeared discontinuities
- via discrete element methods (mainly DEM or DDA) considering several or many discrete discontinuities (joints, interfaces)
- via particle based methods considering different planes of weakness

Numerical simulations are the most complex and most realistic approaches to determine the slope stability. However, the more realistic the model the more information and data are required. The following figures illustrate exemplary the power of numerical simulation techniques to simulate failure pattern of rock slopes.
Fig. 2.5.1 illustrates a typical combined tensile-shear failure of a rock slope via isolines of accumulated shear strain (continuum approach). Fig. 2.5.2 illustrates a plain failure mode along predefined planes of weakness using a discontinuum approach (DEM).

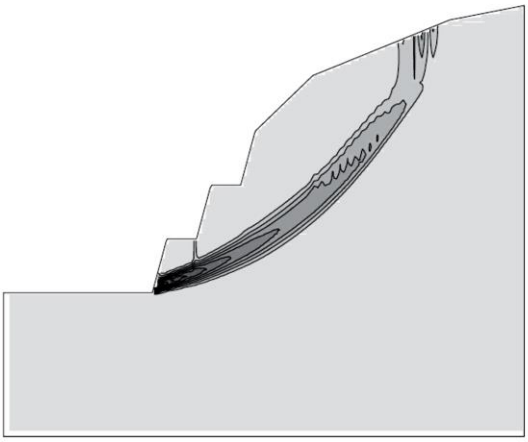

Fig. 2.5.1: Combined tensile-shear failure of a rock slope (Lorig & Varona, 2005)

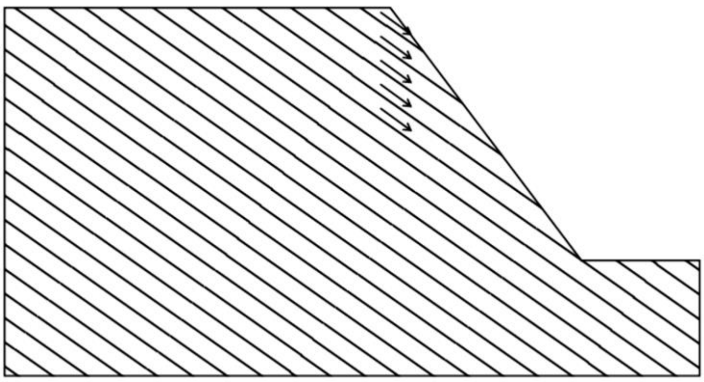

Fig. 2.5.2: Plane failure mode along predefined planes of weakness (Lorig & Varona, 2005)

Fig. 2.5.3 shows two different failure modes: (a) combined failure through rock matrix and along predefined planes of weakness, (b) forward toppling of block structure.

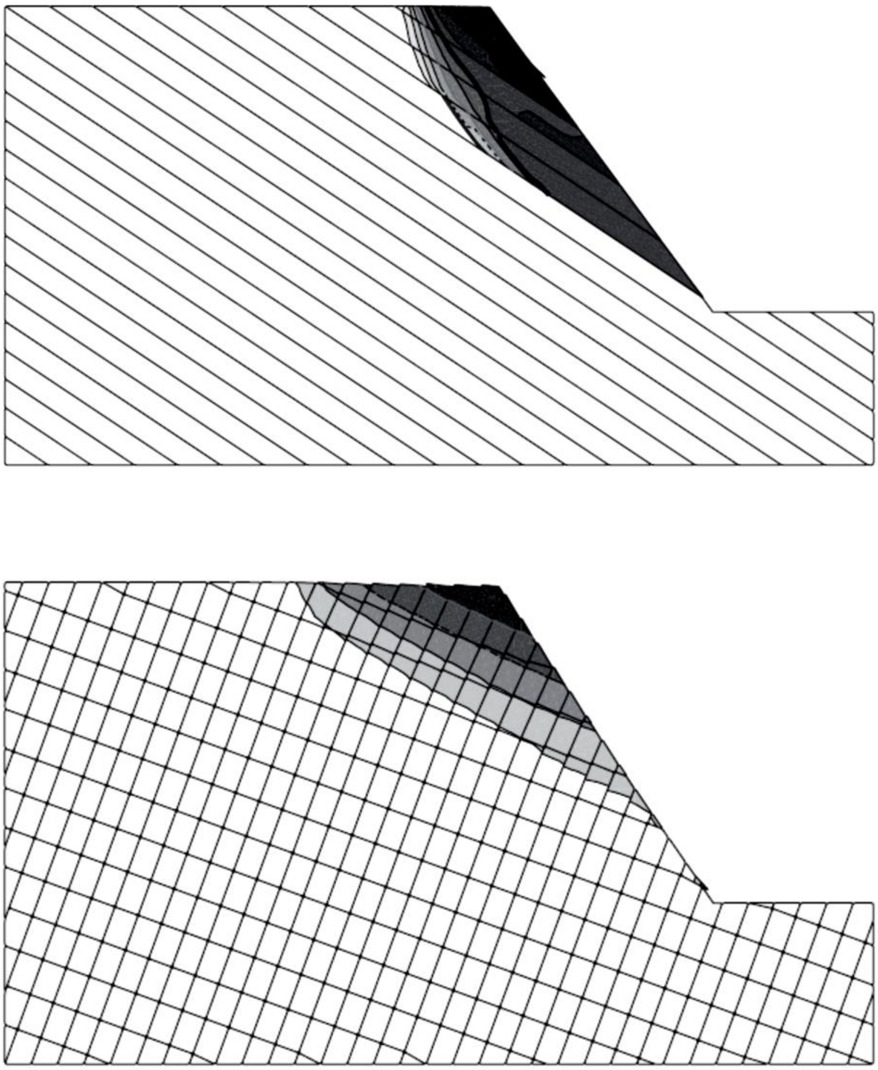

Fig. 2.5.3: Slope failure modes indicated by isolines of horizontal and vertical displacement, respectively (Lorig & Varona, 2005)

Fig. 2.5.4 shows the simulation of a rock slope failure by combining a continuum mechanical approach (FEM) and a discontinuum mechanical approach (DDA).

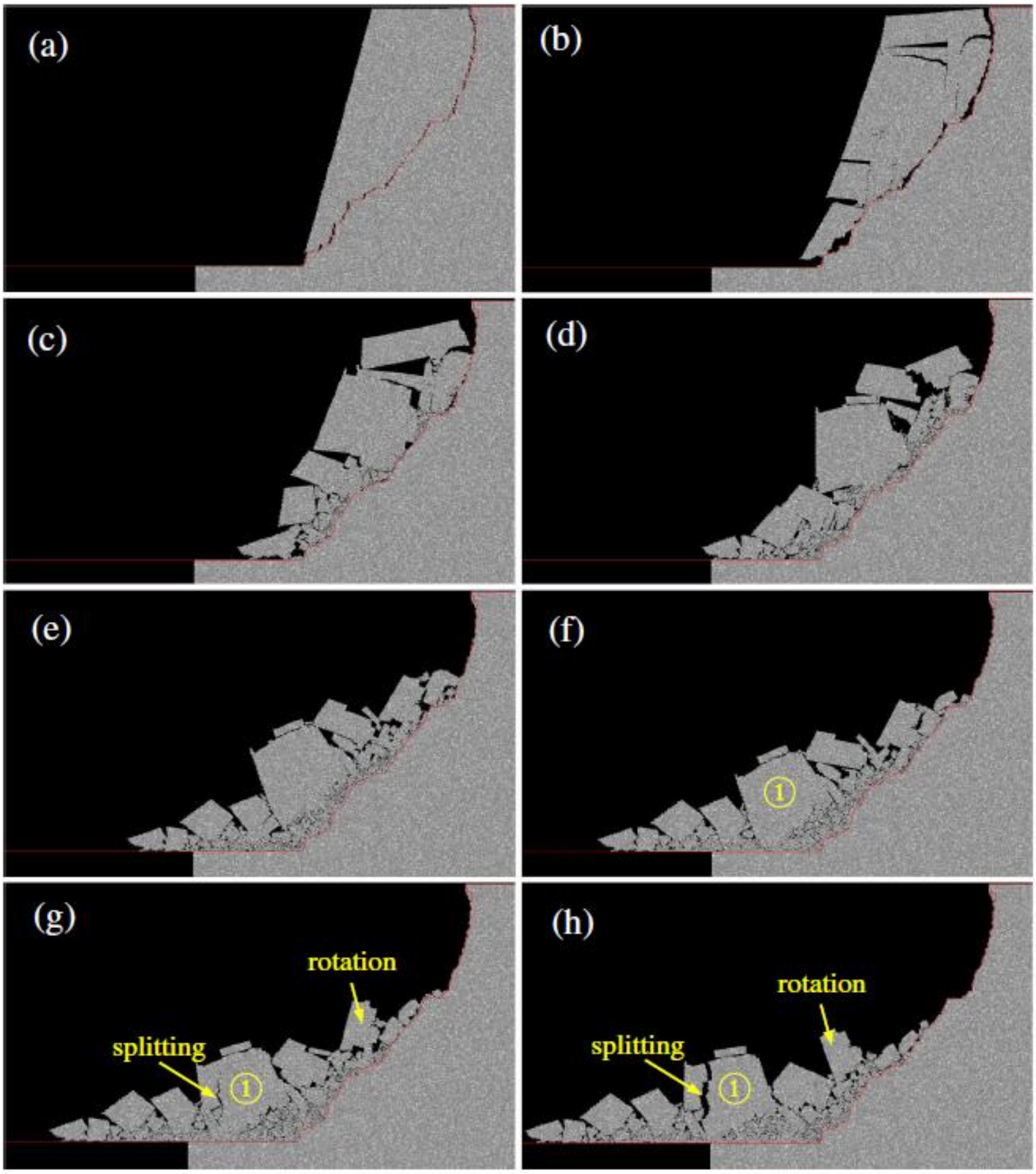

Fig. 2.5.4: Sequence of complex slope failure process and mass movement (Tan et al., 2017)

Fig. 2.5.5 shows a 3-dimensional model of a sandstone massive. By applying the shear- and tensile strength reduction method, factor-of-safety (FOS) values were obtained and potential areas of failure were detected. Different situations (ongoing long-term weathering as well as frost and thaw cycles) were also included in the numerical simulations.

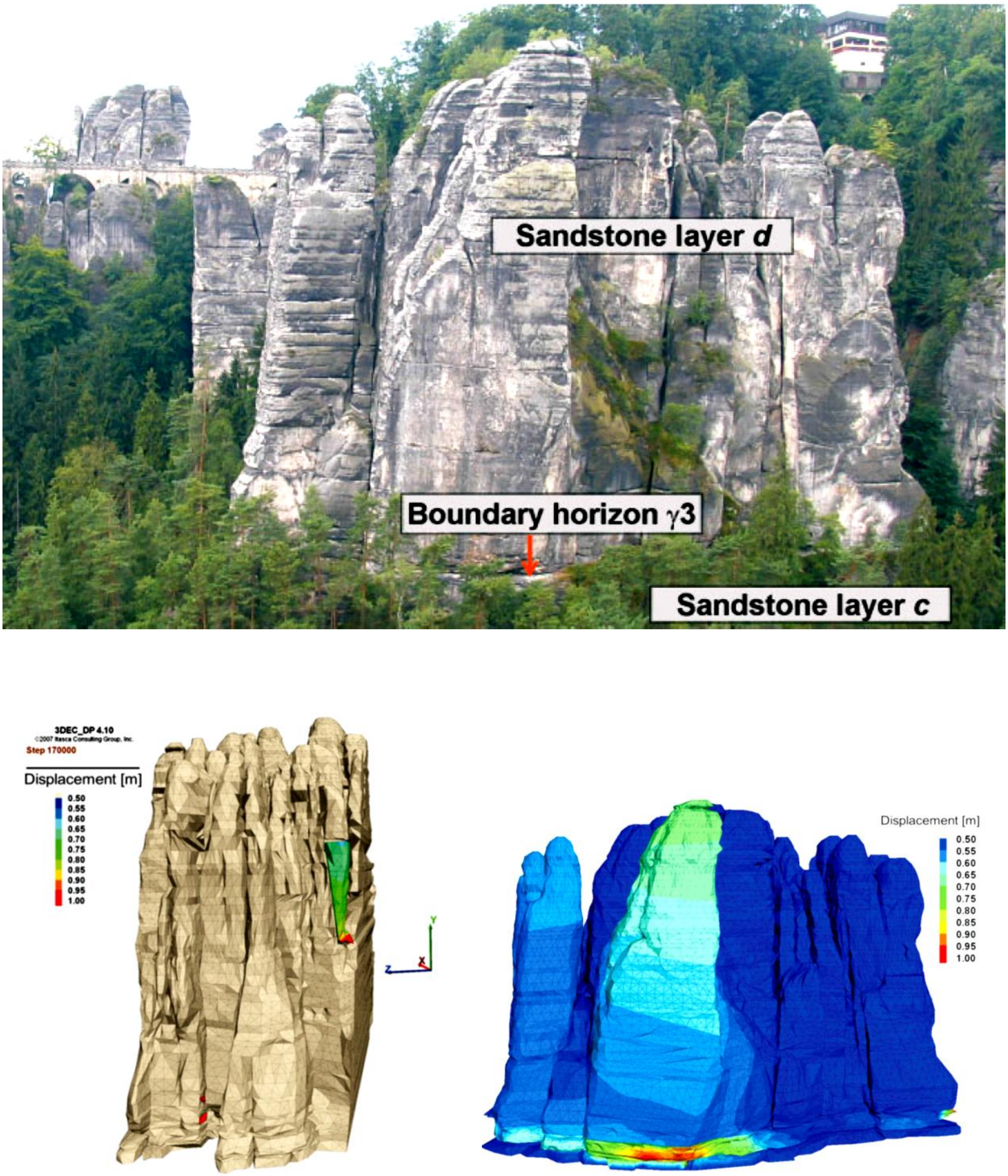

Fig. 2.5.5: Sandstone massive and corresponding numerical models indicating potential areas of failure by large displacements (Herbst & Konietzky, 2017)

3 References

Azarafza, M. et al. (2021): Discontinuous rock slope stability analysis by limit equilibrium approaches – a review, Int. J. Digital Earth, doi: 10.1080/17538947.2021.1988163

Bar, N. & Barton, N. (2017): The Q-slope method for rock slope engineering, Rock Mech Rock Eng., 50: 3307-3322

Basahel, H. & H. Mitri (2017): Application of rock mass classification system to rock slope stability assessment: a case study, J. Rock Mech. Geotechn. Eng., 9: 993-1009

Eberhardt, E. (2003): Rock slope stability analysis – utilization of advanced numerical techniques, https://www.eoas.ubc.ca/personal/erik/e-papers/EE-SlopeStabilityAnalysis.pdf

Haines, A. & Terbrugge, P.J. (1991) Preliminary estimation of rock slope stability using rock mass classifications systems, Proc. 7th Int. Cong. Int. Soc. Rock Mech., Vol. 2: 887-892.

Herbst, M. & Konietzky, H. (2012): Numerical modelling of natural rock formations to estimate stability using the example of a sandstonemassif in Saxony., Geomechanics and Tunneling, 5(4): 379-388

Li, A.J. et al. (2008): Stability charts for rock slopes based on the Hoek-Brown failure Criterion, Int. J. Rock Mech. Min. Sci., 45: 689-700

Lorig, L. & Varona, P. (2005): Numerical analysis, in: Wyllie, D.C. & Mah, C.W. (2005): Rock slope engineering, Spon press, 431 p.

Raghuvanshi, T.K. (2019): Plane failure in rock slopes – a review on stability analysis Techniques, Journal King Saud University, 31: 101-109

Romana, M. et al. (2015): slope mass rating (SMR) geomechanics classification: thirty years review, Proc. ISRM congress 2015, 10 p.

Rusydy, I. et al. (2019): kinematic analysis and rock mass classification for rock slope failure at USAID highways, SDHM, 13(4): 379-399

Sonmez, H & Ulusay, R. (1999): Modifications to the geological strength (GSI) and their applicability to stability of slopes, Int. J. Rock Mech. Min. Sci., 36: 743-760

Stacy, T.R. (2001): Best practice rock engineering handbook for “other” mines, SIMRAC

Taheri, A. & Tani, K. (2007): rock slope design using slope design rating (SSR) – application and field verifications, Proc. ARMA, 2007-027

Tan, S.B. et al. (2017): The failure process analysis of rock slope using numerical simulation techniques, Engineering failure analysis, 79: 999-1016

Wattimena, R.K. (2013): Predicting probability stability of rock slopes using logistic regression, Int. J. JCRM, 9(1): 1-6

Wyllie, D.C. & Mah, C.W. (2005): Rock slope engineering, Spon press, 431 p.